

# Structural and electrical properties of dodecylbenzene sulphonic acid doped polypyrrole/zirconium oxide composites

M. Irfan\* and A. Shakoor

*Department of Physics, Bahauddin Zakariya University, Multan, 60800 Pakistan.*

*\*e-mail: mirfanphysics@gmail.com*

Received 22 April 2019; accepted 28 May 2019

Polypyrrole (PPy) dispersed in organic solvents was synthesized utilizing of dodecylbenzene sulphonic acid (DBSA) as a useful dopant. Composites of doped PPy with DBSA and also mixed with zirconium oxide ( $ZrO_2$ ) nanoparticles were achieved by the chemical polymerization method. Raman spectroscopy has been adopted to confirm the interaction between PPy-DBSA and  $ZrO_2$ . The SEM also confirms the dual-phase structure of platelet and eggshell in PPy-DBSA- $ZrO_2$ . Temperature -dependant DC conductivity exhibited three- dimensional variable ranges hopping (3D-VRH) model. The density of states, hopping length and to activation energy were calculated and it was observed to be effected by increasing the weight ratio of  $ZrO_2$  into PPy-DBSA.

**Keywords:** Polypyrrole; dodecylbenzene sulphonic acid; zirconium oxide composites.

PACS: 75.50.Tt; 81.07.Wx; 61.41.+e; 71.20.Rv.

DOI: <https://doi.org/10.31349/RevMexFis.65.607>

## 1. Introduction

The charge transport mechanism in polymeric materials has been developed increasing part of the research to know about the general theory of polymer physics [1-3]. Conducting polymer / inorganic composites were acquired unique chemical and physical properties and fascinated more attention. Due to exclusive properties conducting polymers have potential applications in materials science and electronics etc. [4-7]. So far many conducting polymers and inorganic nanoparticles have been reported in the literature review [8-10]. Among them,  $ZrO_2$  has potential applications for the fabrications of electronic devices that were described in the literature review [11]. Meanwhile,  $ZrO_2$  was an attractive material with great strength, high thermal stability, low thermal conductivity, and tremendous chemical resistance. These features make the  $ZrO_2$  very important material in the field of temperature- dependent devices applications [12].

The different metals and metal oxide have been encapsulated into conducting polymers, providing a host of composites [11-19]. Among several conducting polymers, PPy is normally known as positive conducting polymers for commercial applications due to high conductivity, simple preparation, and environmental stability but insoluble in organic solvents [20]. An active procedure to reduce this problem is to prepare the composites of conducting polymers doped with a functional dopant such as dodecylbenzene sulphonic acid (DBSA) to minimize the problems of solubility [21-22]. However, the literature review reveals that temperature- dependent DC conductivity studies of PPy doped with DBSA and also mixed with zirconium oxide are scarce. In this article, PPy-DBSA- $ZrO_2$  composites have been synthesized by the chemical polymerization technique that provide unique properties. Temperature dependence DC Conductivity of PPy-DBSA with an increasing ratio of  $ZrO_2$  at different temperatures has been studied. The results cover density of

states, hopping length; activation energy and temperature dependence DC Conductivity were calculated and discussed the acquired results. The charge transport mechanism in these synthesized materials by means of variable range hopping (VRH) model may useful for the fabrication of electronics devices.

## 2. Experimental details

### 2.1. Chemical and materials

The Pyrrole (Fluka) was purified under low pressure and stored at low temperature prior to use. Ammonium Persulphate (APS), Dodecylbenzene Sulfonic Acid (DBSA) and Zirconium oxide ( $ZrO_2$ ) were acquired from Sigma Aldrich also used as obtained. All materials were used as presented without any more purification.

### 2.2. Synthesis of polypyrrole (PPy)

Ammonium Persulphate was isolated in 100 ml of distilled water and stirred for 1h, after that the pyrrole was dissolved gradually into the mixture through stirring at room temperature. The monomer to oxidant molar ratio was retained 1:1. The overall solution was left for 24 h to attain the complete polymerization. Finally, the solution was cleaned and washed with distilled water repeatedly up to the filtrate changes into colorless shape. The greenish-black paste of PPy was achieved which was desiccated at 60°C in a vacuum oven for 24 h.

### 2.3. Synthesis of PPy-DBSA- $ZrO_2$ composites

A total of 0.15 mol of DBSA was dissolved in 100 mL of distilled water, the required mol of Pyrrole was inserted gently into the mixture and the solution was kept on magnetic

stirring. 30 % hydrochloric acid (HCl) was also mixed in it to maintain PH between 0 and 1. To this solution,  $ZrO_2$  powder with increasing weight percentage was added to the polymerization reaction mixture with strong magnetic stirring. After 3 h, the suitable amount of APS was dissolved in 100 mL distilled water then it was mixed dropwise under strong stirring for 1/2 h. The monomer/oxidant/dopant molar ratio was preserved 1:1:1/4. After 24 h, one-liter methanol was also introduced into the reaction mixture. The solution was left for 48 h to achieve complete polymerization. Finally, the solution was rinsed with distilled water continuously until the filtrate changes into colorless shape. The greenish-black paste of PPy-DBSA- $ZrO_2$  was attained which was desiccated at  $60^\circ C$  in a vacuum oven for 24 h.

### 3. Measurements

Raman spectra for 633 nm exciting radiation were detailed on a Renishaw RM 1000 laser Raman (He-Ne laser) obtaining Olympus metallurgical microscope and a CCD detector. The laser power at the sample was retained below  $\sim 0.74$  mW to protect the thermal degradation. The laser was concentrated employing a  $50\times$  objective lens and spatial resolution was concerning  $1\ \mu m$ . Scanning electron microscopy (SEM) was carried out on an EVO50 ZEISS instrument. DC conductivity of all samples was performed with Keithley 2400 electrometers and a current source electrometer by using two probe method.

## 4. Results and discussion

### 4.1. Raman spectroscopy

Raman spectroscopy has been used to quantify the detailed analysis of induced structural changes by adding  $ZrO_2$  in PPy-DBSA. Figure 1a) depicts the Raman spectra of polypyrrole (PPy). The peaks observed at  $1597$  and  $1581\ cm^{-1}$  represent C = C symmetry stretching [23-24]. The two peaks located at  $1314$  and  $1378\ cm^{-1}$  assigned to be the inter ring (C-C) stretching [22-25]. The peak at  $1055\ cm^{-1}$  is attributed to ring deformation and two another peaks were located at  $937$  and  $934\ cm^{-1}$  are seen due to ring deformation related to bipolarons and polarons [26]. Figure 1b) shows the Raman spectra of PPy doped with DBSA. The peak at  $1578\ cm^{-1}$  is observed due to benzenoid C-C ring stretching vibrations and another peak located at  $1601\ cm^{-1}$  showing the quinoid C=C stretching mode of the polymer chain. Figure 1 c)-e) shows that the peaks of PPy-DBSA- $ZrO_2$  composites were found at  $1593\ cm^{-1}$  (N-C stretching band),  $1040\ cm^{-1}$  (N-H in-plane deformation) and  $682\ cm^{-1}$  (C-C out of plane ring deformation). Moreover, two peaks observed at  $607$  and  $574\ cm^{-1}$  are related to benzene ring deformation [27] and cross-linking between the PPy chains [28] respectively. The peak at  $607\ cm^{-1}$  has been attributed to the deformation of the benzene ring in the PPy backbone. Figure 1e)

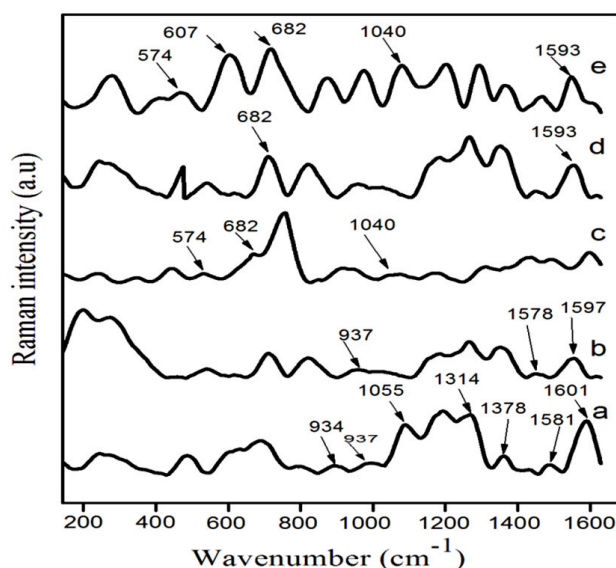


FIGURE 1. Raman spectra of (a) PPy (b) PPy-DBSA (c) PPy-DBSA-2%  $ZrO_2$  (d) PPy-DBSA-4%  $ZrO_2$  (e) PPy-DBSA-8%  $ZrO_2$  composites.

illustrates that the intensity of the peak at  $607\ cm^{-1}$  increases as compared to the peak observed at  $574\ cm^{-1}$  provides information regarding the interactions between polymer components. The literature showing that it was due to the fact that, by inserting  $ZrO_2$  displayed a good attraction between the PPy chains [29]. The relative intensity of the peak at  $607\ cm^{-1}$  indicates that the  $ZrO_2$  mixed with PPy-DBSA confirms the inter chain interaction. This effect was betterly observed in composite an with 8 % weight ratio of  $ZrO_2$  into PPy-DBSA. From this study, it may be concluded that the observed changes in the recorded spectra of new peaks in PPy-DBSA- $ZrO_2$  composites predict the formation of chemical bonding present between PPy-DBSA chains and  $ZrO_2$ .

### 4.2. Scanning electron microscopy (SEM) analysis

The SEM micrograph of pure  $ZrO_2$  nanoparticles and PPy-DBSA- $ZrO_2$  composite can be acquired and are shown in Fig. 2 a)-b). It is clearly observed from the SEM image of polypyrrole (PPy) that it has clusters of spherical shaped particles. At low magnification, SEM of PPy- dodecylbenzene sulphonic acid (DBSA) displays egg shell like surface morphology that may have resulted from phase segregation. The SEM morphology of PPy-DBSA also shows the aggregations of particles which may be due to the increased in inter chain interaction and results to increases the electrical conductivity [30]. At high magnification, SEM image is indicative of hemi spherical nature of polymer as clusters in PPy-DBSA- $ZrO_2$  composite as well as the platelet structure of  $ZrO_2$ . The  $ZrO_2$  nanoparticles are implanted into PPy-DBSA chain because due to the strong particle interaction [31]. From this, it may be concluded that PPy-DBSA- $ZrO_2$  is seeing more growth in particle size and a duel structure of platelet and eggshell.

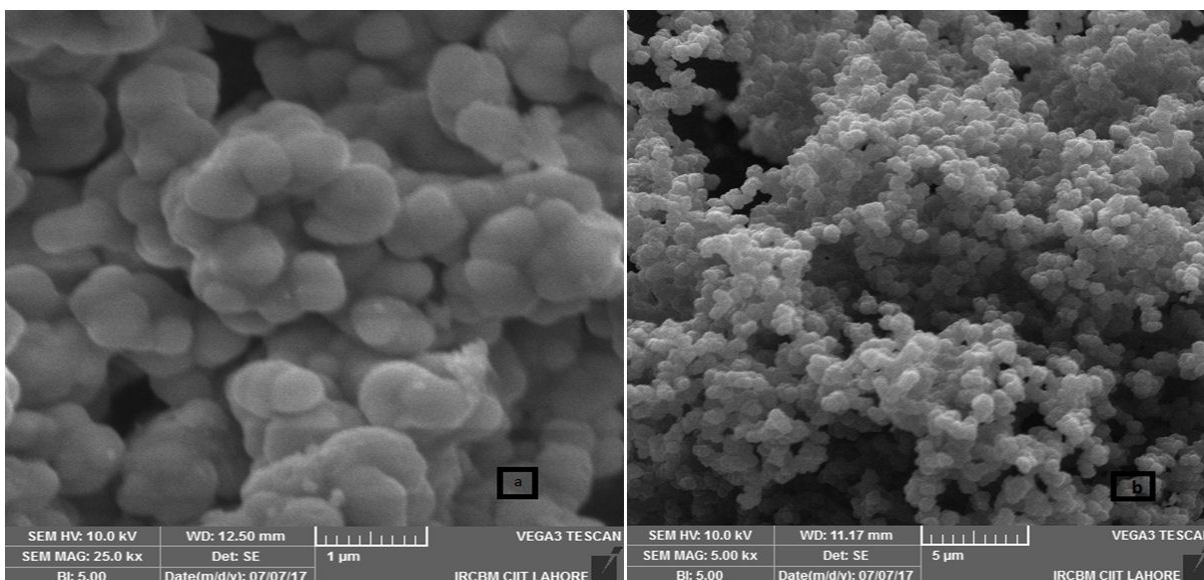


FIGURE 2. SEM micrograph of (a) Pure  $ZrO_2$  (b) PPy-DBSA- $ZrO_2$  composite.

### 4.3. Temperature dependent DC conductivity of PPy-DBSA- $ZrO_2$ composites

#### 4.3.1. Amount of $ZrO_2$ added

A chain of composites with different amount of  $ZrO_2$  (2%, 4% and 8%) were synthesized by retaining the concentrations of pyrrole constant. The different amount of  $ZrO_2$  generates composites of changed conductivity. The conductivities of the composites were found to be decreases with increasing amount of  $ZrO_2$  (Fig. 3). The decrease in conductivity with an accumulation of  $ZrO_2$  may be expected to reducing the conductive pathways because of the insulated nature of  $ZrO_2$ . The accumulation of  $ZrO_2$  reduces degree of conjugated  $\pi$ -bonds in PPy in addition to terminates the ordered structure

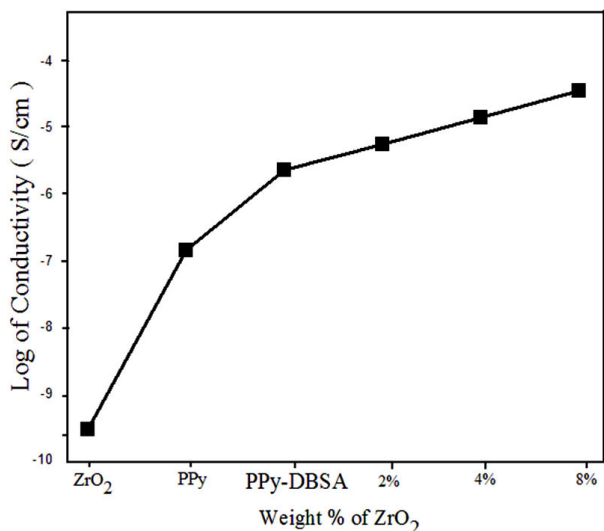


FIGURE 3. The conductivities of PPy-DBSA- $ZrO_2$  composites at different wt % of  $ZrO_2$ .

of polymer chains which effects to decrease in conductivity of the composite. Hence, the existence of  $ZrO_2$  plays a very significant part in the conductivity of PPy-DBSA- $ZrO_2$ .

#### 4.3.2. Temperature dependant DC conductivity

The relation concerning DC conductivity and temperature in the polymer samples can provide imperative information about the nature of phenomena correlated to the charge transport into a polymer system.

$$\sigma = \sigma_0 \exp(-T_0/T)^{1/1+n} \quad (1)$$

Here the exponent  $n$  in Eq. (1) [32-33] is dimensionality of system, its value can be  $n = 1, 2$  or  $3$  for 1-D, 2-D or 3-D VRH charge transport system. The effective dimensionality  $n$  of charge transport based on inter chain coupling. Temperature-dependent Log of conductivity was observed to have a linear relationship to  $T^{-1/4}$  in case of PPy [34], PPy-DBSA and PPy-DBSA- $ZrO_2$  composites. This implies that the charge transport method of these samples follows the 3D variable range hopping (VRH) model. The activation energy is defined as [35].

$$E_a = d(\text{Log}\sigma)/d(1/KT). \quad (2)$$

The differential of the graph of  $\text{Log}\sigma$  vs  $1/kT$  offers activation energy at different temperatures. The Arrhenius exponential law equation is [36].

$$\sigma = \sigma_0 \exp(E_a/KT). \quad (3)$$

By adding Eqs. (2) and (3) we get the following Eq. (4).

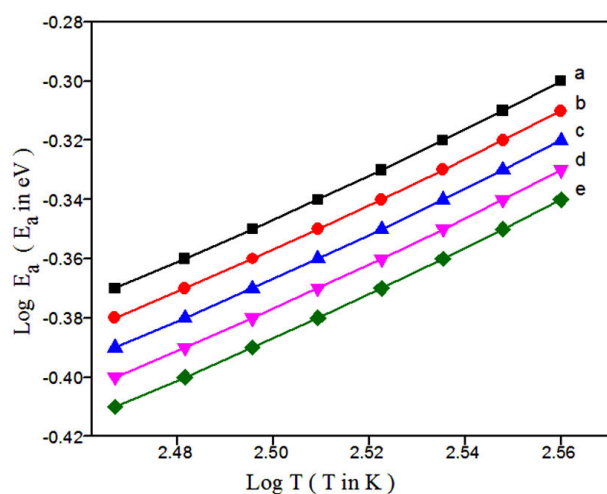
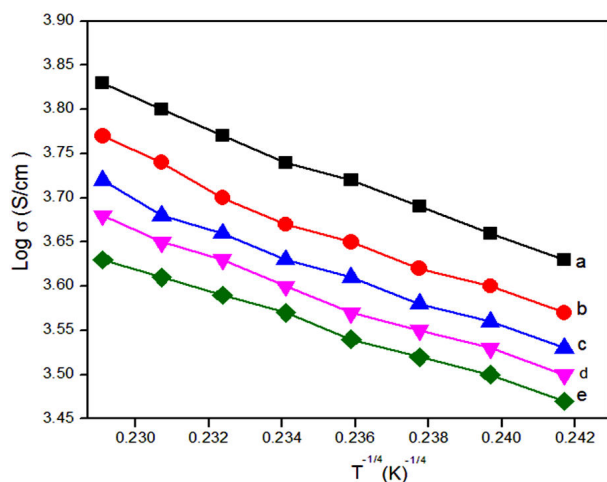
$$E_a = \gamma KT_0(-E_a/KT)^{1/1+n}. \quad (4)$$

Where

$$\gamma = \frac{1}{1+n}. \quad (5)$$

TABLE I. Mott parameters of PPy-DBSA doped with ZrO<sub>2</sub> (2, 4 and 8 %) at 303 K.

Samples	$T_0$ (K)	Density of states $N(E_F)$ ( $\text{eV}^{-1}\text{cm}^{-3}$ )	Hopping length (cm) (R)	Hopping activation energy (eV) (W)	$\sigma_{dc}$ (S/cm)
PPy	$8.14 \times 10^9$	$9.55 \times 10^{23}$	$8.17 \times 10^{-9}$	0.458	$2.3 \times 10^{-4}$
PPy-DBSA	$8.05 \times 10^9$	$9.66 \times 10^{23}$	$8.12 \times 10^{-9}$	0.456	$2.64 \times 10^{-4}$
PPy-DBSA-ZrO <sub>2</sub> (2%)	$5.02 \times 10^9$	$1.54 \times 10^{24}$	$7.25 \times 10^{-9}$	0.407	$2.77 \times 10^{-4}$
PPy-DBSA-ZrO <sub>2</sub> (4%)	$5.38 \times 10^9$	$1.44 \times 10^{24}$	$6.15 \times 10^{-9}$	0.414	$3.14 \times 10^{-4}$
PPy-DBSA-ZrO <sub>2</sub> (8%)	$3.52 \times 10^{-9}$	$2.21 \times 10^{24}$	$6.63 \times 10^{-9}$	0.372	$3.38 \times 10^{-4}$

FIGURE 4. Graph of  $\text{Log } E_a$  vs  $\text{Log } T$  for (a) PPy (b) PPy-DBSA (c) 2% (d) 4% (e) 8% ZrO<sub>2</sub> in PPy-DBSA.FIGURE 5. DC conductivity ( $\sigma_{DC}$ ) as a function of  $T^{-1/4}$  in a logarithmic scale for (a) PPy ( $y = -15.60x + 7.39$ ,  $R^2 = 0.996$ ), (b) PPy-DBSA ( $y = -15.56x + 7.32$ ,  $R^2 = 0.983$ ), (c) PPy-DBSA-2% ZrO<sub>2</sub> ( $y = -14.46x + 7.06$ ,  $R^2 = 0.989$ ), (d) PPy-DBSA-4% ZrO<sub>2</sub> ( $y = -14.06x + 6.89$ ,  $R^2 = 0.992$ ), (e) PPy-DBSA-8% ZrO<sub>2</sub> ( $y = -12.64x + 6.52$ ,  $R^2 = 0.997$ ).

This activation energy may also be misused to see the charge transport hopping mechanism. Temperature dependent exponent  $n$  of either equal to 0.25 [37-39] or 0.5 [40-42] for various morphologies of conducting polymers. For strong inter chain coupling, exponent  $\gamma$  is 0.25 and effective dimensionality  $n = 3$  for temperature dependent DC conductivity data will follow a 3D-VRH model. For weak inter chain coupling, VRH exponent is 0.5 ( $n = 1$ ) which could describe in terms of a granular metal model or quasi 1D [43] or Afros' Shklovskii [44] VRH models. For PPy-DBSA-ZrO<sub>2</sub> by plotting  $\text{Log}(E_a)$  vs  $\text{Log}T$  (Fig. 4) a straight line of slope  $\{-(\gamma - 1)\}$  equal to 0.756 is obtained which resembles the hopping exponent  $\gamma \sim 0.25$  and  $n \sim 3$ . This confirms that 3D-VRH dominates the mechanism of charge transport in PPy-DBSA-ZrO<sub>2</sub> composite same as 3D-VRH model apply in PPy [34]. The activation energy attained from Arrhenius plot increases with increase in temperature. Therefore,  $\text{Log}(\sigma)$  having linear relationship with  $T^{-1/4}$  as shown in Fig. 5. From these results, we observed that strong inter chain interaction present in PPy-DBSA as well as in PPy-DBSA-ZrO<sub>2</sub> samples. But decrease in DC conductivity of clay sample is due to insulating behavior of ZrO<sub>2</sub> nanoparticles [45].

## 5. Conclusions

The composites of doped Polypyrrole (PPy) with Dodecylbenzenesulphonic acid (DBSA) and also mixed with ZrO<sub>2</sub> nanoparticles were synthesized by chemical polymerization technique. The structural properties of synthesized samples were studied by Raman spectroscopy. SEM micrographs show that the composites are in the form of extended chains and increase in the particles size as compared with PPy and ZrO<sub>2</sub> is also observed. The addition of ZrO<sub>2</sub> disturbed the delocalization of charge carriers and decrease the inter chain interaction due to which DC conductivity of PPy-DBSA-ZrO<sub>2</sub> ( $\sigma_{dc} = 3.38 \times 10^{-4}$  S/cm at room temperature) is higher as compared to PPy-DBSA ( $\sigma_{dc} = 2.64 \times 10^{-4}$  S/cm at room temperature). Temperature dependant DC conductivity displayed three dimensional variable ranges hopping (3D-VRH) model. Density of states, hopping length, and activation energy were calculated and seen to be changed by growth of ZrO<sub>2</sub> into PPy-DBSA.

1. K. Dutta and S. K. De, *J. Nanoparticle Res.* **9** (2007) 631
2. E. Vitoratos, S. Sakkopoulos, E. Dalas, P. Malkaj, and C. Anestis, *Curr. Appl. Phys.* **7** (2007) 578
3. T. K. Vishnuvardhan, V. R. Kulkarni, C. Basavaraja, and S. C. Raghavendra, *Bull. Mater. Sci.* **29** (2006) 77
4. R. Gangopadhyay and A. De, *Chem. Mater.* **12** (2000) 608
5. X.W. Li, G.C. Wang and X.X. Li, *Surf. Coat. Technol.* **197** (2005) 56
6. D. J. Cardin, *Adv. Mater.* **14** (2002) 553
7. L.J. Zhang and M.X. Wang, *J. Phys. Chem.* **107** (2003) 6748
8. M. Skunik, M. Chojak, I. A. Rutkowska and P. J. Kulesza, *Electrochim. Acta.* **53** (2008) 3862-306
9. H.F. Guo, H. Zhu, H.Y. Lin and J.Q. Zhang, *Mater.Lett.* **62** (2008) 2196
10. H. Sertchook and D. Avnir, *Chem. Mater.* **15** (2003) 1690
11. Guohui Tian, Kai Pan, Honggang Fu, Liqiang Jing, Wei Zhou, *J. Hazard. Mater.* **166** (2009) 939-944
12. B. Basu, *Int. Mater. Rev.* **50** (2005) 239-256
13. N. Parvatikar, S. Jain, C.M. Kanamadi, and M.V.N.A. Prasad Sens, *Actuators B Chemical* **114** (2006) 599
14. M. Nagaraja, J. Pattar, N. Shashank, J. Manjanna and H.M. Mahes, *Synth. Met.* **159** (2009) 718
15. Y. Mtsuo, S. Higashika, K. Kimura, Y. Miyamoto and Y. Sugie *J. Mater. Chem.* **12** (2002) 1592
16. J. Jiang, L.H. Ai, D.B. Qin, H. Liu and L.C. Li, *Synth. Met.* **159** (2009) 695
17. D.C. Schnitzler, M.S. Meruvia, I.A. Hqmmelgen and A.J.G. Zarbin, *Chem. Mater.* **15** (2003) 4658
18. C.C. Zeng, X.M. Han, L.J. Lee, K.W.Koelling and D.L. Tomasko, *Adv. Mater.* **15** (2003) 1743
19. S.K. Dhawan, K. Singh, A.K. Bakhshi and A. Ohlan, *Synth. Met.* **159** (2009) 2259
20. G. Jiang, M. Gilbert, D. J. Hitt, G. D. Wilcox, and K. Balasubramanian, *Composites, Part A: Appl. Sci.* **75** (2002) 677
21. M. Compos, F. R. Simon, and E. C. Pereira, *Sens. Actuators B* **125** (2007) 158
22. D. Y. Kim, J. Y. Lee, C. Y. Kim, E. T. Kang, and K. L. Tan, *Synth. Met.* **72** (1995) 243
23. Y.C. Liu, B.J. Hwang, *Synth. Met.* **113** (2000) 203-207
24. Y.C. Liu, K.H. Yang, L.H. Lin, J.F. Tsai, *Electrochim. Commun.* **10** (2008) 161-164
25. M. Grzeszczuk, A. Kepas, C. Kvarnstrom, A. Ivaska, *Synth Met.* **160** (2010) 636-642
26. K. Crowley, and J. Cassidy, *J. Electroanal. Chem.* **547** (2003) 75-82
27. M.J. Santos, A.G. Brolo, E.M. Girotto, *Electrochim. Acta.* **52** (2007) 6141-6145
28. P. Kathuroju, and N. Jampana *IEEE Sens. Appl. Symp.* **1** (2011) 163-166
29. M. Tagowska, B. Palys, K. Jackowska, *Synth. Met.* **142** (2004) 223
30. Basavaraja C, Jo EA, Kim BS, Kim DG, Huh DS. *Macromol. Res.* **11** (2010) 1037-1044
31. M. Irfan, A. Shakoor, A. Majid, N. Hassam, and N. Ahmed, *Polymer Science Series A* **61** (2019) 105-111
32. Y. Ward, Y. Mi, *Polymer.* **40** (1999) 2465
33. J. Dyre, *J Appl. Phys.* **64** (1988) 2456
34. A. Shakoor, T. Zahra Rizvi, H. Umer Farooq, N. Hassan, A. Majid and M. Saeed *Polymer Science Series* **53** (2011) 540-545
35. N.F. Mott, *Electronic Process in Non-crystalline Materials.* **1** (1979) 1
36. E. Schmidbauer and P. Schmid-Beurmann *J. Solid State Chem.* **177** (2004) 207-215
37. F. Zuo, M. Angelopoulos, A. G. MacDiarmid and A.J. Epstein, *Phys. Rev. B.* **39** (1989) 3570
38. R. Singh, J. Kumar, R. K. Singh, S. Chand and V. Kumar, *J. Appl. Phys.* **100** (2006) 505-572
39. J. Joo *et al.*, *Synthetic Metals*, **84** (1997) 83
40. J. Joo, J. K. Lee, J. S. Baeck, K. H. Kim, E. J. Oh and J. Epstein, *Synthetic Metals* **117** (2001) 455
41. A. Wolter, P. Rannou, J. P. Travers, B. Gilles and D. Djurado, *Phys. Rev.* **58** (1998) 7637
42. Z. H. Wang, E. M. Scherr, A.G. MacDiarmid and A. J. Epstein, *Phys. Rev.* **45** (1992) 4190
43. T. Hu and B.I. Shklovskii, *Phys. Rev.* **74** (2006) 054205
44. D.S. Maddison and T. L. Tansley, *J. Appl Phys.* **72** (1992) 4677
45. B. R. Saunders, K. S. Murray and R. J. Flemming, *Synthetic Metals* **47** (1992) 167